Acta Crystallographica Section A
Foundations of Crystallography
ISSN 0108-7673

Received 28 April 2004
Accepted 5 August 2004

Structural phase transitions from and to the quasicrystalline state

Walter Steurer

Laboratory of Crystallography, Department of Materials, ETH Zurich, CH-8093 Zurich, Switzerland, and MNF, University of Zurich, Switzerland. Correspondence e-mail: steurer@mat.ethz.ch

Phase transitions from and to the quasicrystalline state show a typical signature due to some structural peculiarities. Both quasicrystals and most of their translationally periodic transformation products, the approximants, consist of the same basic structural units ('clusters'). This is the cause of low-energy interfaces between the newly forming phase and the parent phase. It is also the origin of the rather high stability of the frequently resulting orientationally twinned nanodomain structures. Owing to topological incompatibilities between quasiperiodic and periodic structures, purely displacive phase transitions are impossible. Diffusion of a significant fraction of atoms, at least on the scale of the cluster diameters, always has to take place. Locally similar icosahedral structural ordering between parent phase and nucleating phase is also responsible for the frequently occurring formation of icosahedral quasicrystals from undercooled liquid alloys or during devitrification of metallic glasses. The different types of experimentally observed phase transitions are discussed, from amorphous to quasicrystalline, quasicrystalline to ordered/disordered quasicrystalline and quasicrystalline to crystalline as a function of temperature, pressure, irradiation and high-energy ball milling, respectively.

1. Introduction

Are quasicrystals (QC) just entropy-stabilized high-temperature (HT) phases or are they stable down to 0 K, *i.e.* are QC a new ground state of matter alternative to periodic crystals? This is still an open question. In the first case, there must be a phase transition from the QC to the stable periodic low-temperature (LT) phase. Consequently, the study of structural phase transitions from and to the quasicrystalline state is not only of interest on its own but also from a more general viewpoint. However, structural LT phase transitions of intermetallics are experimentally difficult to investigate owing to their sluggish kinetics if atomic diffusion is involved. Therefore, methods enhancing diffusion of atoms such as irradiation by high-energy electrons or ions are of particular interest.

Is there anything special about phase transitions of QC? Do they differ in any way from those of translationally periodic crystals (PC) or those of incommensurately modulated structures (IMS), the other large class of aperiodic crystals (*cf.* Cummins, 1990)?

An IMS can be considered as resulting from a 1D, 2D or 3D displacive and/or substitutional modulation of an underlying periodic basic structure. The periods of the modulation wave and of the basic structure are incommensurate to each other. The modulation wavevector may continuously vary with temperature or pressure running through all rational and irrational multiples of the lattice parameters. If the amplitude of the modulation wave approaches zero, the periodic average structure (PAS) of the IMS continuously turns into the basic structure without any variation in the equilibrium positions of the atoms. The unit cell of a PAS results from projecting the infinite IMS into the unit cell of the basic structure.

Typically, IMS transform by a second-order phase transition into a HT high-symmetry periodic structure. The order parameter of this transition can be related to the amplitude of the modulation wave, which decreases with increasing temperature. The phase transition can be well described in terms of the phenomenological Landau theory (see, for instance, Bak, 1982). At low temperature, IMS often undergo a soft-mode-driven lock-in transition to a periodic phase (the irrational wavevector locks in a rational value), which can be described as a commensurately modulated phase (superstructure).

Geometrically, QC can be described in different ways depending on what property is to be discussed. Starting from its reciprocal-space image, for instance, it can be considered as a composite structure of mass density waves with wavevectors locked by the constraints of non-crystallographic symmetry (Bak, 1985). Phenomenologically, infinitesimal distortions (linear phason strain) of the wavevectors (reciprocal lattice) could create a devil's staircase of phase transitions running through all orders of rational approximants as it is known from IMS (Bak, 1982). This has never been observed for QC transitions, however.

A rational approximant of a QC consists of the same building units ('clusters') as the QC, its structure is periodic,

however. Based on the higher-dimensional approach (see, for instance, Steurer & Haibach, 1999*b* or 2001, and references therein), a quasiperiodic structure can geometrically be transformed into its rational approximant by a continuous rotation of the d-dimensional (dD) cutting space $V^{\parallel}$ (physical, parallel or external space) or by a shear (linear phason strain) of the nD hypercrystal structure parallel to the $(n-d)$D perpendicular (or complementary or internal) space $V^{\perp}$. For icosahedral quasicrystals, $n = 6$, for octagonal, decagonal and dodecagonal quasicrystals, $n = 5$, respectively, and in all these cases $d = 3$. In the case of icosahedral and decagonal phases, the basis vectors of the nD hypercrystal structure have irrational components related to the 'golden mean'

$$\tau = \lim_{n\to\infty} \frac{F_{n+1}}{F_n} = \frac{1+5^{1/2}}{2} = 2\cos\left|\frac{\pi}{5}\right| = 1.618\ldots$$

with the Fibonacci numbers F_n, with $F_{n+2} = F_{n+1} + F_n$ and $F_0 = 0$, 0, $F_1 = 1$. A rational $\langle F_n, F_{n+1}\rangle$ approximant is obtained if in the vector components τ is replaced by the ratio of two Fibonacci numbers (there are different notations in use, however).

If projected onto a unit cell of appropriate dimensions, one obtains the PAS of a QC (Steurer, 1999). In the nD description, this corresponds to an oblique projection of the hypercrystal structure onto the parallel space. In the case that the QC and its transformation product have the same PAS, the displacive part of the phase transition can take place quite rapidly leading to a chemically disordered intermediate state.

A distortion (disorder) of the hypercrystal structure is called phonon-like if it takes place parallel to the physical space, phason-like if it only extends along the perpendicular space. The distortions may be linear or non-linear, isotropic or anisotropic. Random phason fluctuations can be described by a phason Debye–Waller factor in analogy to the Debye–Waller factor related to random phonon fluctuations. In the 3D reciprocal space, increasing linear phason strain manifests itself in a continuous displacement of the reflections from their original high-symmetry positions on a Z-module of rank n. In direct space, linear phason strain causes atomic jumps (phason flips) transforming a quasiperiodic structure into a periodic one. The practical problems related to this mechanism have been discussed by Steurer (1999, 2000*b*, and references therein).

A more physical description of QC is based on atomic clusters. The term cluster will be used in the meaning of a fundamental structural unit building both QC and their approximant crystals (AC). It is still not fully clear whether or not these clusters are just coordination polyhedra such as the octahedra in the NaCl structure, for instance, or subunits, which are stabilized electronically ('magic numbers') or by covalent bonding contributions.

Despite some similarities between QC and IMS (*cf.* Steurer, 2000*b*, and references therein) such as the (lock-in) transformation to rational approximants, there are also major differences: the wavevectors of the mass density waves do not continuously vary with temperature; QC do not transform to periodic HT high-symmetry phases in second-order transitions; purely displacive QC–AC transitions are not possible owing to topological incompatibilities (Duneau & Oguey, 1990*a*); equilibrium can be easily achieved during IMS transitions contrary to the much more sluggish QC transitions.

The literature on phase transitions from and to the quasicrystalline state is scattered over hundreds of publications. To my knowledge, no comprehensive general review on this topic has ever been published. There is just one slim book containing a collection of papers on different aspects of QC phase transitions (Yacaman & Torres, 1993), and one chapter in a book on the theory of reconstructive phase transitions (Toledano & Dmitriev, 1996).

In the following, a short review is given on experimentally observed phase transitions from and to quasiperiodic structures with eightfold, tenfold and icosahedral diffraction symmetry (*i.e.* octagonal, decagonal or icosahedral phases), respectively. Theoretical interpretations and models are given wherever they already exist. The review is by no means complete either in the experimental or in the theoretical section. It just presents typical examples of the different types of QC phase transformations observed to date.

2. Experimentally observed transformations from and to the quasicrystalline state

Only a few fully reversible structural phase transitions of QC as a function of temperature or pressure have been reported so far. Most of them are transitions between different quasiperiodic ordering states. Quite common, however, are QC–PC transformations taking place under irradiation or during high-energy ball milling. These transitions are usually accompanied by, or rather a consequence of, an induced change in chemical composition (morphotropic transition). Remarkably, even in these cases, characteristic orientation relationships between special directions in the QC and the transformation product are found. Also frequently observed is the formation of mostly metastable QC during devitrification of amorphous alloys (*a* alloys). These *a* alloys have been found to undergo a two-stage phase transition during annealing. First, in the LT regime, a metastable quasicrystalline phase nucleates. Later on, at HT, this QC phase is transformed into a crystalline phase.

2.1. Amorphous to quasicrystalline to crystalline

Supercooled liquid alloys. The nucleation rate of the icosahedral phase (*i* phase) in undercooled liquid alloys is extremely high (*cf.* Holzer & Kelton, 1993; Kelton, 2004; and references therein). This indicates a very low interfacial energy between the quasicrystalline nuclei and the liquid and, consequently, a locally similar structural ordering. Since an icosahedron consists of 20 slightly distorted tetrahedra and has locally a higher packing density than the cubic and hexagonal close sphere packings, the existence of local icosahedral (polytetrahedral) ordering in undercooled liquids has already been suggested by Frank (1952). Recently, some more experimental evidence for Frank's hypothesis was found in an undercooling experiment on liquid $Ti_{39.5}Zr_{39.5}Ni_{21}$. At 953 K,

first a metastable *i* phase formed, which a few seconds later transformed into the Laves phase that is stable at this temperature (Kelton *et al.*, 2003). Since the *i* phase is stable only below 843 K, the nucleation barrier for the *i* phase must be significantly lower than for the Laves phase, which also shows local polytetrahedral order. This small interfacial energy seems also to play an important role for the frequently observed QC nucleation in amorphous alloys.

a-$Zr_{65}Ni_{10}Cu_{7.5}Al_{7.5}Ag_{10}$. The phase transitions of $Zr_{65}Ni_{10}Cu_{7.5}Al_{7.5}Ag_{10}$ bulk metallic glass were studied by continuous heating and isothermal annealing (Liu & Chan, 2004). Activation energies for QC nucleation were found with 280 kJ mol^{-1}, significantly smaller than the 366 kJ mol^{-1} reported for rapidly quenched amorphous ribbons. This indicates a local structure that is closer to icosahedral order in the bulk metallic glass than in the amorphous ribbon. The Avrami exponent varied from 3 to 2 as a function of the already transformed volume fraction of the sample. This was interpreted by a mechanism of 3D interfacial-controlled growth with zero-nucleation rate followed by diffusion-controlled growth with changing nucleation rate and, finally, a 2D interfacial-controlled growth with grain-edge nucleation. At higher temperatures, the quasicrystalline phase transformed into a crystalline Zr_2Cu-like phase.

The influence of pressure on the amorphous-to-quasicrystal transition was investigated on a material with the same composition by *in situ* high-pressure (0.68 GPa) and HT (663 – 693 K) X-ray diffraction as a function of annealing time (Jiang *et al.*, 2001). The Avrami exponent was determined to be the very low value of 1, indicating that atomic diffusion may play an important role in this phase transition. Indeed, the main effect of pressure was to enhance the onset temperature for the formation of QC with a rate of 9.4 K GPa^{-1} while the temperature interval for the stability of QC and their grain size decreased.

a-Al–Cu–V, a-Al–Cu–Ti. A somewhat different transformation path was found in the case of melt-spun amorphous Al–Cu–V and Al–Cu–Ti alloys (Misra *et al.*, 2003). In the first stage of annealing, Al_2Cu nucleates. In the second stage, the remaining amorphous alloy transforms to the *i* phase and α-Al. Nanocrystalline Al_2Cu may provide sites for heterogeneous nucleation of the icosahedral phase.

Heating up *a*-$Al_{75}Cu_{15}V_{10}$ obtained by high-energy ball milling transformed it to an icosahedral QC in a first exothermic reaction (727 K). After a second exothermic reaction (794 K), the *i* phase transformed to crystalline Al_3V and Al_2Cu (Asahi *et al.*, 1994). The structure of *i*-$Al_{75}Cu_{15}V_{10}$ prepared by annealing amorphous starting material of the same composition was interpreted, based on X-ray diffraction peak-width data, by the icosahedral glass model (Tsai *et al.*, 1987, 1994).

2.2. Quasicrystalline to crystalline

This kind of transition requires an extensive reconstruction of the structure, which needs diffusion of atoms. At temperatures $T < T_m/2$, *i.e.* well below the melting temperature T_m, this can only be achieved if the sluggish phase-transition kinetics is enhanced by ballistic diffusion associated with a high defect density. This is the case during high-energy electron or ion irradiation as well as during high-energy ball milling, respectively. In these cases, it is probable, however, that, owing to induced changes in chemical composition, the transitions are morphotropic rather than polymorphic.

2.2.1. As a function of temperature. *i-Al–Cu–Fe(Si).* Several transitions of the *i* phase have been observed depending on sample composition and annealing conditions: QC to cubic $\langle 1,1\rangle$ (Quivy *et al.*, 1996) and rhombohedral $\langle 2,1\rangle$ (Audier *et al.*, 1991), $\langle 3,2\rangle$ (Liu *et al.*, 1991) or $\langle 5,3\rangle$ approximants (Liu & Köster, 1993). In some cases, an intermediate linear-phason strained quasicrystalline phase or a transient modulated *i* phase with satellite reflections along the fivefold directions was observed (Audier *et al.*, 1991). According to Audier *et al.* (1993), the transition *i* phase (stable at $T > 948$ K) to rhombohedral approximant (stable at $T < 948$ K) is reversible. Heating up as-quenched samples of the *i* phase leads first to the formation of the modulated *i* phase ($673 < T < 923$ K, in some experiments up to 1023 K) with the modulation period ($\approx$200 Å) increasing with temperature. A symmetry analysis for the modulated quasicrystal using a 12D superspace group was performed in terms of the Landau theory (Perez-Mato & Elcoro, 1994). For longer annealing times ($873 < T < 923$ K), the system transforms into a two-phase system with chemical composition fluctuations (Menguy *et al.*, 1992) as well as with phason and phonon disorder (Menguy *et al.*, 1993). Longer annealing at $943 < T < 953$ K recovers a well defined *i* phase and a rhombohedral approximant in coexistence.

This behaviour was successfully modelled by free-energy analysis in terms of composition and phason strain (Waseda *et al.*, 1994). In agreement with the experimental evidence, the calculated phase diagram shows the HT *i* phase and the LT approximant separated by a two-phase region with both phases coexisting. By taking into account the energy associated with the phason strain gradient, spatially fluctuating phason strain should be present in the two-phase region (*i.e.* a modulated transient phase). In their previous experimental work, Waseda *et al.* (1993) found that at the composition $Al_{63}Cu_{24}Fe_{13}$ the *i* phase has its largest stability range as a function of temperature ($730 < T < T_m$). They calculated a hypothetical order/disorder transition temperature of 1590 K (melting temperature $T_m \approx 1100$ K) based on the intensity evolution with temperature of the superstructure reflections (related to *F*-centring of the 6D Bravais lattice). The rhombohedral $\langle 2,1\rangle$ approximant was obtained for compositions $Al_{64}Cu_{24}Fe_{12}$–$Al_{63}Cu_{26}Fe_{11}$, the rhombohedral $\langle 3,2\rangle$ approximant for slightly lower Al concentration such as $Al_{62}Cu_{26}Fe_{12}$. The intermediate state ($Al_{63}Cu_{25}Fe_{12}$, 943 K) was interpreted by a slope of the strip in the 6D approach equal to 1.70–1.75 (in the ideal QC it amounts to $\tau = 1.618\ldots$).

The transition from the as-quenched icosahedral phase to the cubic $\langle 1,1\rangle$ approximant, α-$Al_{55}Cu_{25.5}Fe_{12.5}Si_7$, takes place within 2 h at 823 K almost without any change in chemical composition (Le Lann & Devaud, 2000). A theoretical model for the transition mechanism based on the domain structure

observed was suggested. The domains, each one containing a few cubic approximant unit cells, are assumed to already exist in the parent *i* phase. They act as nuclei for the formation of the cubic α phase. The translation vectors connecting them are therefore still vectors of the *i* phase and 'the extension of the periodic structure needs a partial reconstruction between joining domains . . . '. The authors point out that this occurs by 'small rearrangements' of atoms rather than by a 'reconstructive transformation' (Duneau & Oguey, 1990*b*; Le Lann & Devaud, 2000).

i-Ti–Zr–Ni. The phase stability of icosahedral $Ti_{41.5}Zr_{41.5}Ni_{17}$ was studied by Yi & Kim (2000). The best way to produce the *i* phase is by melt spinning and subsequent annealing. It transforms above 838 K to the body-centred cubic *W* phase, a $\langle 1,1\rangle$ approximant. By cooling, the reverse transformation could not be observed probably due to the sluggish kinetics.

i-Mg–Zn–Al. After heating a mechanically alloyed sample of *i*-$Mg_{44}Zn_{41}Al_{15}$ to temperatures above 613 K, it transformed topotactically to the metastable cubic $\langle 2,1\rangle$ approximant. Cooling the sample down yielded the icosahedral phase again (Bokhonov *et al.*, 2000). It should be kept in mind that mechanical alloying leads to highly defective samples.

i-Zn–Mg–Y. A reversible phase transition between *i*-$Zn_{64}Mg_{27}Y_9$ (20 h at 873 K) and hexagonal *h*-$Zn_{66}Mg_{27}Y_7$ (72 h at 773 K) was observed during annealing experiments by Abe & Tsai (1999). The hexagonal phase was found to be structurally related but not a rational approximant. At 750 K, both phases exist adjacent to each other in the phase diagram.

d-Al–Co–Cu–Si. A synchrotron-radiation diffraction study of the microcrystalline state of a slowly cooled sample with composition $Al_{63}Co_{17.5}Cu_{17.5}Si_2$ was performed by Fettweis *et al.* (1994). They discussed structure models of twinned approximants of the type $a = b = 51.515$, $c = 4.13$ Å, $\gamma = 108^\circ$. In an *in situ* high-temperature study on samples with the same composition, it was found that a reversible QC–AC transformation takes place at ≈1023 K (Fettweis *et al.*, 1995). The observed hysteresis indicates a first-order transition. Denoyer *et al.* (2000) identified as-grown (Bridgman technique) samples as an orientationally twinned 1D QC. The transformation of this state to the decagonal phase (*d* phase) took place at ≈1103 K. In neither study have transient states (such as in a 'devil's staircase' known from IMS) been observed.

d-Al–Co–Ni. Eight different structural modifications of the decagonal phase were identified by electron-microscopic methods, which were called 'basic Ni-rich', 'basic Co-rich', 'superstructure type I (S1 + S2)', 'superstructure type I (S1)', 'superstructure type II', '1D quasicrystal', 'LT pentagonal phase' 'HT pentagonal phase' (Ritsch *et al.*, 1998). It is not clear whether or not all of them are stable.

A 'continuous' transformation between the decagonal quasicrystalline and the crystalline state was observed by electron-microscopic investigations of differently long annealed (1120–1370 K, 40–1370 h) samples with composition $Al_{72.7}Co_{19}Ni_{8.3}$ (Döblinger *et al.*, 2002). After homogenization, the *d* phase with S1 superstructure was identified as a minority phase beside a disordered quasiperiodic phase with pseudo-fivefold symmetry and without superstructure reflections. By prolonged annealing, these phases were transformed into a 1D QC and finally to a 'non-Fibonacci-type approximant' (for a definition of this term, see Döblinger *et al.*, 2002) with lattice parameters $a \approx 50.8$, $b \approx 8.25$, $c \approx 32.2$ Å.

Metastable i-Al–(Mn, Fe)–(Si). Metastable QC show rather short correlation lengths of a few hundred Å at most, *i.e.* a few cluster diameters only. Additionally, they contain many defects and may not be fully chemically ordered. Consequently, the diffusive transition to crystalline phases will be easier than that of perfectly ordered stable quasicrystals.

As an example, for this kind of transition, the transformation of metastable *i*-$Al_{80}Mn_{20}$ into a crystalline phase *via* a *d* phase is discussed. A melt-spun ribbon consisting of ≈93% dendritic *i* phase was heated *in situ* in the electron microscope (Kim *et al.*, 1990). First, the non-equilibrium α-Al was consumed during growth of the *i* phase, and then at ≈773 K heterogeneous nucleation of facetted *d* phase took place at the cost of the completely consumed *i* phase. At 873–928 K, the *d* phase transformed rapidly into a crystalline phase (λ- or μ-Al_4Mn).

A different transition pathway, probably due to the higher Al content (Kimura *et al.*, 1986) was found for rapidly quenched *i*-$Al_{85}Mn_{14}Si_1$ and *i*-$Al_{85}(Mn_{0.72}Fe_{0.28})_{14}Si_1$ (Pannetier *et al.*, 1987). Besides other methods, *in situ* powder neutron diffraction experiments were performed and evaluated based on the contrast variation method. Both samples were heated directly up to 700 K, and both were transformed into their orthorhombic modifications, *o*-Al_6Mn and *o*-$Al_6(Mn_{0.72}Fe_{0.28})$. In the *in situ* experiment, a first step starts at ≈620 K and is completed at ≈690 K with the formation of the orthorhombic phase. The second step starts at ≈710 K with the formation of the cubic α-Al–Mn–Si phase and ends at ≈750 K. Based on contrast variation data, the authors conclude that the Al subnetwork of the *i* phase transforms smoothly into that of the orthorhombic phase 'without deep modification of the subset average structure'. On the contrary, the Mn subnetwork is completely reconstructed, 'the Mn subnetwork destabilizes when the Al subnetwork has absorbed too much external aluminium'.

Metastable d-Al_5Pd. A comprehensive study of metastable *d*-Al_5Pd and its structural transitions as a function of temperature was performed by Ma *et al.* (1990). On heating to 873 K for several hours, the *d* phase gradually transforms into decagonally twinned orthorhombic Al_3Pd and into τ phases.

Metastable octagonal phases. The phase transition of the metastable melt-spun octagonal phase *o*-$Mn_{82}Si_{15}Al_3$ to either cubic microtwinned $Mn_3Si(Al)$ (slow heating) or a β-Mn-type (rapid heating) structure was discussed by Xu *et al.* (2000). The transitions are described phenomenologically as being of the phason type and resulting from two different phason fields.

A continuous change from metastable *o*-Cr–Ni–Si and *o*-Mn–Si–Al to the cubic phase with β-Mn structure type was observed by moving the SAED (selected-area electron diffraction) aperture successively from the octagonal to the cubic area of the samples (Wang & Kuo, 1990). The orientational relationship between the cubic and the octagonal

phase resulted in $[001]_{\beta\text{-Mn}} \parallel [00001]_{\text{octagonal}}$ and $[100]_{\beta\text{-Mn}} \parallel [11000]_{\text{octagonal}}$ (Li & Cheng, 1996).

The transformation was explained by gradual introduction of a phason strain field (Mai *et al.*, 1989). A theoretical model for this transition based on the Schur rotation (*i.e.* a one-parameter rotation in the *n*D description) was published by Baake *et al.* (1991).

2.2.2. Under irradiation. By fast particle irradiation of a sample above a specific energy (20–30 eV), threshold radiolytic (ionization and bond breaking) or knock-on (collision and knocking out of atoms from their sites) damage can take place. Radiolytic effects predominantly occur at low energies, knock-on effects only at high energies. The induced defects accelerate atomic diffusion considerably (Gittus, 1978; Smith, 1997). This may help to overcome the sluggish kinetics of low-temperature QC–PC transformations.

i-$Al_{62}Cu_{25.5}Fe_{12.5}$. The irradiation-induced (120 keV Ar^+ ions) dose-dependent transition to the *B*2 phase (CsCl-type) of *i*-$Al_{62}Cu_{25.5}Fe_{12.5}$ was studied at room temperature (RT) (Wang *et al.*, 1993) and at liquid-nitrogen temperature (Yang *et al.*, 1996). The orientation relationship between the fivefold (*A*5) and twofold (*A*2) direction of the QC and the corresponding directions of the *B*2 phase observed was: $A5 \parallel [110]_{B2}$, $[113]_{B2}$, $A2 \parallel [11\bar{1}]_{B2}$. Heating the irradiated and transformed sample in the electron microscope above 880 K yielded the *i* phase back again. Below 880 K, it remained in the *B*2 phase. This was taken as evidence that the *B*2 phase is the stable phase at RT.

The effect of irradiation with 900 MeV Pb and 780 MeV Xe ions of *i*-$Al_{62}Cu_{25.5}Fe_{12.5}$ and structurally related cubic α-$Al_{55}Cu_{27}Fe_{11}Si_7$ was studied at 80 K and at RT by high-resolution X-ray diffraction (Coddens *et al.*, 2003). This experiment was complementary to the above-mentioned one due to the different energy deposition by the ions in the target, *i.e.* mainly by high electronic excitations instead of by nuclear collisions. While for the cubic phase almost no variation was observed in shape and position of Bragg peaks, for the *i* phase significant peak broadening and a slight peak-position shift was measured. Since no characteristic correlation with the perpendicular-space component of the diffraction vector was found, the authors conclude that the defects induced are of non-phasonic origin. The relaxation of the energy deposited in the excited electrons is assumed to generate shock waves with pressures of several tens of GPa. Since quasicrystals seem to be remarkably stable under pressure, it is not surprising that no phase transition was observed in this experiment.

d-Al–Co–Cu(–Si, Ge). A first electron-microscopic study on *d*-$Al_{65}Co_{15}Cu_{20}$ in a sample orientation showing one quasiperiodic and the periodic direction was performed by Reyes-Gasga *et al.* (1992). They reported that irradiation of the *d* phase with a 400 kV electron beam induced a structural transformation, which cannot be observed for beams with 100 kV, for instance. In a similar experiment, Zhang & Urban (1992) showed that *d*-$Al_{65}Co_{20}Cu_{15}$ and *d*-$Al_{62}Co_{15}Cu_{20}Si_3$ first transform into the β phase (disordered CsCl-type), which then orders into a CsCl-type phase. The total time for the transformation was 15 min for an electron current density of 10^{23} electrons s^{-1} m^{-2}. The authors concluded that the transformation was not induced by electron beam heating ($\Delta T <$ 323 K) but by radiation damage, and that the major effect consisted in an enhancement of the rate at which the transformation occurred. The stable phase at room temperature should be the CsCl-type one, consequently. The orientation relationship between the *d* phase and the cubic phase was as follows: $A10 \parallel [110]$, $A2D \parallel [1\bar{1}0]$ or $[1\bar{1}1]$, $A2P \parallel [001]$ (*A*2*P* and *A*2*D* denote the two symmetrically inequivalent twofold directions). Song *et al.* (1993) observed lattice fringes in an as-cast $Al_{65}Co_{15}Cu_{25}$ alloy, indicating an orientationally twinned crystalline nanodomain structure. Twinning was also visible in electron diffraction patterns. After annealing for 500 h at 1073 K, the sample did not show any lattice fringes, indicating a *d* phase; the electron diffraction pattern exhibited perfect tenfold symmetry. The orientation relationship and the partial lattice match between *d*-Al–Co–Cu and the CsCl-type Al–(Co, Cu) phase was discussed in great detail by Song *et al.* (1996).

A QC–PC transformation was observed during electron-beam irradiation of a microcrystalline sample with composition $Al_{63}Co_{17.5}Cu_{17.5}Si_2$ (Audier & Robertson, 1991). The transformation from the microcrystalline to the quasiperiodic state takes place shortly before the sample begins to melt. Irradiation experiments carried out later on microcrystalline $Al_{62}Co_{15}Cu_{20}Si_3$ with a 400 keV electron beam confirmed this phase transformation (Reyes-Gasga *et al.*, 1995).

The orientation relationship between the *d* phase and the β phase was explained in terms of the PAS common to both phases (Steurer, 2000*a*). The $[\bar{1}10]_\beta$ direction of the β phase is parallel to the tenfold axis of the decagonal QC, $[110]_\beta$ and $[111]_\beta$ are parallel to the two different twofold axes of the *d* phase. From this it follows for the average structure: $\mathbf{a}_1^{AS} \parallel [001]_\beta$, $\mathbf{a}_2^{AS} \parallel [110]_\beta$ and $\mathbf{a}_3^{AS} \parallel [\bar{1}10]_\beta$. The translation period along $[001]_\beta$ ranges from 2.88 to 2.92 Å, along $[110]_\beta$ and $[\bar{1}10]$ from 4.08 to 4.13 Å, respectively, for lattice parameters of the β phase from a_β = 2.88 Å in the case of AlCo to a_β = 2.92 Å in the case of Al(Co, Cu). This fits nicely with the periods in the respective directions of the periodic average structure of the *d* phase (Al–Co–Cu: $a_r = 2.436$, $a_1^{AS} = 2.88$, $a_2^{AS} = 3.96$, $a_3^{AS} = 4.15$ Å; Al–Co–Ni: $a_r = 2.456$, $a_1^{AS} = 2.90$, $a_2^{AS} = 3.99$, $a_3^{AS} = 4.08$ Å).

Under irradiation with 1.5 MeV Xe^+ ions, *d*-Al–Co–Cu–Ge transformed into an Al-depleted b.c.c. phase (β phase?) and an amorphous phase of the same composition as the original *d* phase (Chen *et al.*, 1997). After the irradiation dose had been increased, the sample became fully amorphous. Annealing at temperatures above 430 K led to nucleation of the *d* phase again. Final annealing at 873 K restored the complete diffraction pattern of the original *d* phase.

d-Al–Co–Ni. The phase transformations of annealed $Al_{70}Co_{15}Ni_{15}$ under irradiation with a 120 keV Ar^+ ion beam were studied by electron diffraction (Qin *et al.*, 1995). The following transformation sequence was observed as a function of increasing dose: ordered *d* phase ⇒ disordered *d* phase ⇒ b.c.c. phase (β phase?) ⇒ CsCl-type phase ⇒ b.c.c. phase (β phase?). First, the increasing number of defects leads to an

increase in disorder accompanied by diffusion of atoms to approach the equilibrium structure. Then, owing to the high concentration of defects, thermal diffusion leads to an ordered (close to equilibrium) state. Finally, further irradiation destroys the ordered equilibrium phase again.

i-Al$_{70}$Pd$_{20}$Mn$_{10}$. Under 1.5 keV Ar$^+$ irradiation, the pentagonal surface of icosahedral $Al_{70}Pd_{20}Mn_{10}$ transforms into the cubic β phase (Bolliger *et al.*, 1998). Annealing at 700 K restores the icosahedral symmetry again. Both phases are in an orientation relationship with a high degree of structural registry. The authors find 'most remarkable ... the long-range orientational coherence across the entire macroscopic surface of both the b.c.c. and annealed quasicrystalline structures'. The fivefold axis of the *i* phase perpendicular to the surface is parallel to the [110] direction of the β phase. This case is very similar to the example discussed above since the pentagonal surface of the *i* phase is similar to that of a *d* phase.

2.2.3. By high-energy ball milling. After up to 30 h high-energy ball milling, *d*-$Al_{65}Co_{15}Cu_{20}$ was found to be fully transformed to a rather disordered nanocrystalline *B*2 phase. Annealing up to 150 min at 873 K resulted in an increased ordering of the *B*2 phase rather than in the back-transformation to the decagonal phase (Mukhopadhyay, Murthy *et al.*, 2002*a*,*b*). It is unclear whether this is due to different resulting chemical composition of the *B*2 phase compared with that of the original *d* phase.

After 1 h high-energy (attritor) ball milling of *i*-$Al_{63}Cu_{26}Fe_{11}$ (under air), it was partly transformed to the *B*2 phase (Mukhopadhyay, Yadav & Srivastava, 2002). Further milling for 10 h yielded the nanocrystalline *B*2 phase in an amorphous matrix. Subsequent heating/cooling cycles in a differential thermal analysis (DTA) experiment lead to a partial restoration of the *i* phase while annealing at 1123 K for 10 to 20 h yields just well ordered *B*2 phase. Somewhat milder conditions during ball milling (under argon) of *i*-$Al_{65}Cu_{20}Fe_{15}$ lead to a purely amorphous phase (Nasu *et al.*, 1992). No *B*2 phase was observed at any time in this experiment.

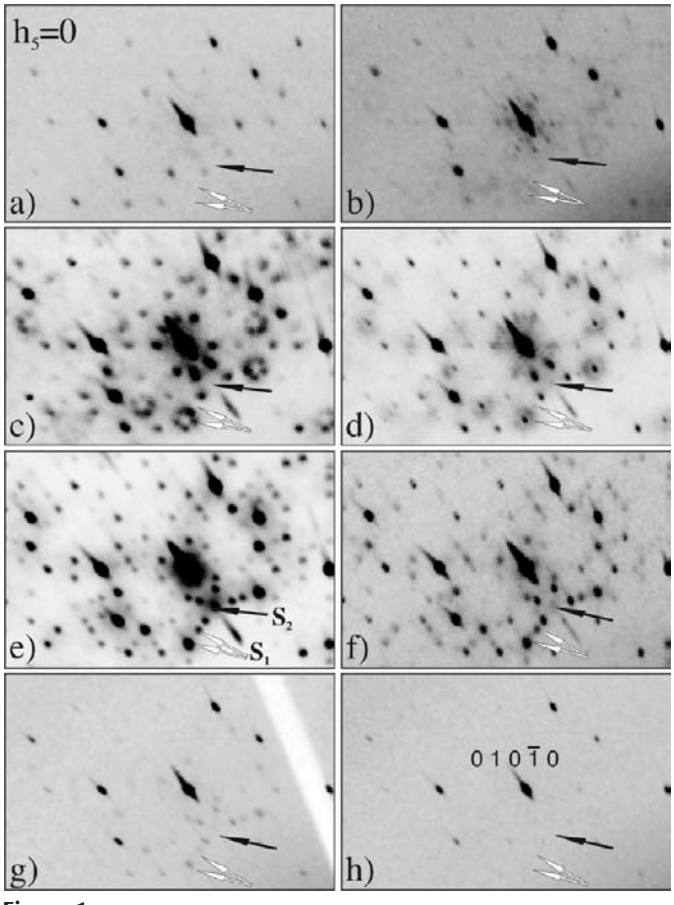

Figure 1
Example of morphotropic phase transitions in the stability range of decagonal Al–Co–Ni. Enlarged area around the strong 01$\bar{1}$0 reflection of decagonal Al–Co–Ni across its stability field (at 1173 K). Positions of S1 and S2 superstructure reflections of the type I phase are marked by white and black arrows, respectively. (*a*) 'Basic Co-rich' $Al_{72.5}Co_{19.5}Ni_8$, (*b*) $Al_{71.5}Co_{18}Ni_{10.5}$, (*c*) $Al_{71.5}Co_{16}Ni_{12.5}$, (*d*) $Al_{71.5}Co_{15}Ni_{13.5}$, (*e*) 'superstructure type I (S1 + S2)' $Al_{71.5}Co_{14}Ni_{14.5}$, (*f*) 'superstructure type I (S1)' $Al_{71.5}Co_{10.5}Ni_{18}$, (*g*) $Al_{71.5}Co_{10}Ni_{18.5}$, (*h*) 'basic Ni-rich' $Al_{71.5}Co_{8.5}Ni_{20}$.

2.3. Quasicrystalline to ordered/disordered quasicrystalline

Several examples of ordering transitions have been observed for icosahedral and decagonal QC, respectively. The transitions may occur either as a function of composition (morphotropic) (Fig. 1) or as a function of temperature (polymorphic) (Fig. 2).

i-Al$_6$Li$_3$Cu. Pressure-induced amorphization was found for *i*-Al_6Li_3Cu above $\approx$10 GPa. At higher pressures, above $\approx$28 GPa, a quasicrystalline (?) phase was formed again (Akahama *et al.*, 1989). The authors interpreted it in analogy to the well known b.c.c.-to-f.c.c. high-pressure transformation as a transition from an *i* phase based on triacontahedral clusters to one built from clusters of the Mackay type.

i-Al$_{71}$Mn$_8$Pd$_{21}$. The temperature-induced reversible phase transitions of *i*-$Al_{71}Mn_8Pd_{21}$ were studied by Hirai *et al.* (2000), Letoublon *et al.* (2000) and De Boisseu *et al.* (1998). It

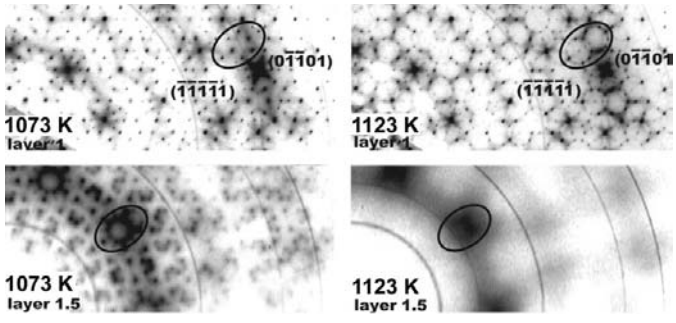

Figure 2
Example of a polymorphic phase transition, superstructure type I (S1 + S2) to superstructure type I (S1), for *d*-$Al_{70}Co_{12}Ni_{18}$. Reciprocal-space sections $h_1h_2h_3h_4h_5$ are shown, with $h_5 = 1$ and 1.5 based on $a_5^* = 4.08$ Å, collected at 1073 and 1123 K, respectively, which have been reconstructed from 360 image-plate scanner frames at each temperature (*marresearch* 345, wavelength $\lambda = 0.7$ Å, oscillation angle $\Delta\phi = 0.5^\circ$, Swiss Norwegian Beam Lines/ESRF, Grenoble). Regions encircled show typical changes in the intensities of S1 and S2 satellite reflections and diffuse scattering phenomena. The basis of Steurer & Haibach (1999*b*) was used for indexing.

was found that the HT *F* phase, an ordered icosahedral phase with *F*-centred 6D hypercubic structure (a_F = 12.901 Å), is stable above 1021 K. At annealing temperatures between 1009 and 981 K, the *F*2 phase is formed within a few minutes. The *F*2 phase is a superstructure of the *F* phase, which can be described in terms of a 6D diamond structure (Ishimasa, 1995). It has been shown by *in situ* single-crystal neutron diffraction that this phase is not a stable but rather a transient state between the *F* phase and the $F2_M$ phase (Letoublon *et al.*, 2000). The $F2_M$ phase is a modulated quasicrystalline phase with just cubic diffraction symmetry representing a superstructure of the *F*2 phase (Audier *et al.*, 1999). At the locations of the superstructure reflections of the $F2_M$ phase, there is already diffuse scattering in the *F*2 phase. The *F*2-to-$F2_M$ phase transition takes around 10 h at 1011 K indicating a diffusion-controlled mechanism (see also De Boissieu *et al.*, 1998).

i-Al$_{63.5}$*Cu*$_{24}$*Fe*$_{12.5}$. *i*-Al–Cu–Fe was reported to transform to a rhombohedral crystalline state *via* an intermediate modulated quasicrystalline phase, with modulation periods varying with temperature (Audier *et al.*, 1990, 1991; Janot *et al.*, 1991). The transition from the icosahedral QC to the modulated intermediate state was modelled by a mechanism based on fractional shears of the 6D hypercrystal (Duneau & Oguey, 1991; Duneau, 1992). A characteristic network of domains bounded by planar defects results from bounded transformations mapping the 6D QC lattice onto a lattice for which the physical space is rational. The Fourier transform of this structure shows satellite reflections of the type that has been experimentally observed. Audier *et al.* (1991) suggest a detailed model with a periodic phason mode, which finally locks into the crystalline approximant. Such a type of second-order transition, driven by a soft phason mode instability, was discussed by several groups (Bancel, 1989; Ishi, 1990, 1992; Janssen, 1991). Menguy *et al.* (1992) pointed out that, however, a chemical composition variation could also drive such a transition. Indeed, in the experimental study of *i*-$Al_{63.5}Cu_{24}Fe_{12.5}$, they verified qualitatively that the modulation is thermally activated, and that atomic diffusion should be involved in the phase transition. They also found a compositional variation of the Al and Fe concentration of approximately ±1.5%.

According to an X-ray diffraction study on *i*-$Al_{63.5}Cu_{24}Fe_{12.5}$ by Denoyer *et al.* (1993), the satellite peaks of the modulated transient state are arranged along the 12 fivefold axes with a distance from the main reflections of 0.0066 Å^{-1} (this corresponds to a modulation wavelength of 151.5 Å). They conclude that there is no experimental evidence for the assumption that the resulting orientationally twinned rhombohedral phase corresponds to a lock-in transition of the modulated QC state in the classical meaning of IMS phase transitions. Another *in situ* X-ray diffraction study on *i*-$Al_{63.3}Cu_{23.4}Fe_{13.3}$ showed that decreasing the temperature from 1073 K causes increasing diffuse scattering finally peaking to satellite reflections below ≈913 K (Boudard *et al.*, 2000). At ≈903 K, Bragg reflection splitting indicates the formation of a microcrystalline state.

d-Al–Co–Ni. An ordering transition in *d*-Al–Co–Ni was discovered by Edagawa *et al.* (1994). By single-crystal X-ray diffraction on annealed $Al_{70}Co_{13}Ni_{17}$, the temperature dependence was measured of the intensities of main reflections and first- and second-order satellite reflections of the 'superstructure type I (S1 + S2)'.

An *in situ* HT X-ray diffraction study on *d*-$Al_{70}Co_{12}Ni_{18}$, quenched from 1173 K, was performed by Steurer *et al.* (2001). Between 1073 and 1123 K, the correlation length related to the diffuse interlayers is drastically decreased and the S2 superstructure reflections become weaker (Fig. 2). The S1 reflections and the main reflections with large perpendicular space component, however, even increase their intensities within a certain temperature range supporting the random tiling picture.

An *in situ* HT study ($290 \leq T \leq 1100$ K) by dilatometry and powder X-ray diffraction was performed on annealed polycrystalline *d*-$Al_{71.2}Co_{12.8}Ni_{16}$ (Soltmann *et al.*, 2003). The 'type I' ⇔ 'S1' phase transition was identified to be of second order with an onset temperature of 1007 K and a finishing temperature of 1042 K. It is accompanied by an elongation of coordination polyhedra along the tenfold axis and a contraction perpendicular to it. Thermal expansion was found to be isotropic at temperatures up to 900 K. The mobility of atoms was estimated based on diffusion coefficient data. Within 100 s, Co and Al move ≈0.8 and ≈20 Å at 670 K, ≈18 and ≈350 Å at 770 K, respectively.

The same ordering transition was studied in *d*-$Al_{71.5}Co_{14.5}Ni_{14}$ by means of positron lifetime and coincident Doppler-broadening measurements (Sato *et al.*, 2004). Significant changes in the temperature dependence of these two parameters were discovered at 650 and at 1140 K. The reversible phase transition at 650 K was observed for the first time. It was assumed to result from the change from an Ni-rich vacancy surrounding to more Co or a small addition of Al. A change in the slope of the temperature dependence of the quasilattice parameter was also observed around 650 K by Soltmann *et al.* (2003). The transition at 1140 K was related to well known 'type I' ⇔ 'S1' phase transition. The state at 650 K could be quenched contrary to that at 1140 K. At 650 K, the mean diffusion length of Co was estimated to be 10–20 Å on a time scale of 10^5 s.

A LT study was performed on slowly cooled *d*-$Al_{70.7}Co_{13.3}Ni_{16.0}$, milled 2 min in a ball mill (Kupsch *et al.*, 2002*a*,*b*). X-ray powder diffractograms were taken *in situ* in the temperature range $100 \leq T \leq 200$ K. At ≈150 K, additional reflections appeared. The phase transition was found to be reversible but subjected to fatigue. No LT transition could be observed on single- or polycrystalline samples of similar composition by Hassdenteufel *et al.* (2004).

2.4. Phase transitions of rational approximants

Phase transitions of rational approximants are of interest since they are built from the same fundamental clusters as the QC they are related to. A phenomenological study in terms of the Landau theory was performed of the possible phase

transitions in cubic approximants of *i* phases (Chizhikov, 1999). Thereby, it was assumed that the number of atoms in the unit cell does not change during the transition. Only order/disorder transitions were considered and the results demonstrated on transitions in the $\langle 0,1\rangle$ approximant (FeSi-type structure) based on sublattice ordering.

Cubic cI168-Cd_6Me (Me = Ca, Y, Yb). *c*-Cd_6Y, a $\langle 1,1\rangle$ approximant of icosahedral *i*-$Cd_{5.7}Yb$ and *i*-$Cd_{17}Ca_3$, shows a LT phase transition at 164 K. The transition is believed to be due to the ordering of the innermost shell of the basic 66-atom icosahedral cluster occupying the vertices and body centre of the cubic unit cell. The innermost cluster, a Cd_4 tetrahedron in the centre of a Cd_{20} dodecahedron, is orientationally disordered above 164 K. At lower temperatures, the ordering is accompanied by a very small tetragonal distortion and the formation of a $2 \times 2 \times 1$ orthorhombic (?) superstructure (Tamura *et al.*, 2003). A similar order/disorder transition was found for isotypic *c*-Cd_6Yb at about 110 K (Tamura *et al.*, 2002).

Cubic R-Al_5Li_3Cu. Contrary to the behaviour of *i*-Al_6Li_3Cu, which shows at $\approx$23 GPa a reversible transition to an unknown crystalline (?) phase (Sadoc *et al.*, 1996), cubic *R*-Al_5Li_3Cu transforms into the amorphous state at a similar pressure (Winters & Hammack, 1993). Pressure-induced, largely isoconfigurational, amorphization indicates locally close structural (topological) relationship of the two ordering states such as polytetrahedral packing.

3. Microscopic models for the transition quasicrystal to approximant

The QC-to-AC transition was discussed in several papers employing the formalism of the Landau theory, *i.e.* deriving the symmetry groups of the transformation products by symmetry analysis of the parent phase. The symmetry changes $D_8 \Rightarrow D_4$, $D_{10} \Rightarrow D_2$, $D_{12} \Rightarrow D_6$ and $D_{12} \Rightarrow D_4$ for possible QC-to-AC transitions caused by linear phason strain have been derived and analysed (Hu *et al.*, 1996). The non-vanishing phason strains have been determined and the corresponding rational approximants derived.

The structural instabilities driven by soft phason modes in icosahedral QC were studied by Ishi (1992). He found three distinct soft modes causing the symmetry changes $I_h \Rightarrow D_{5d}$, $I_h \Rightarrow D_{3d}$ and $I_h \Rightarrow C_{2h}$. Locking in the phason strain related to $I_h \Rightarrow D_{3d}$ leads to a twinned rhombohedral AC similar to that observed experimentally (Ishi, 1990).

The QC-to-AC transition in terms of the Landau theory was discussed in the example of the Fibonacci chain and the Penrose tiling (Beraha *et al.*, 2001). The basic idea behind this model was to describe QC as IMS by shearing the hypercrystals along the parallel space in an appropriate way (Steurer, 2000*b*). In analogy to the well developed Landau theory for IMS, the formalism for QC was deduced.

Phenomenologically, the phase transitions from and to the quasicrystalline state are much better understood and simpler to describe than their mechanism on the microscopic scale. Microscopic models for QC-to-AC transitions are usually based on defect-free perfectly ordered quasiperiodic structures of the type that can be properly described in the higher-dimensional approach. Real QC, however, seem to possess structural perfection at best on a global average rather than locally. There are strong indications of intrinsic structural substitutional disorder accompanied by relaxation of the atoms coordinating the substituted sites (see, *e.g.*, the results of quantitative QC structure analyses reviewed by Steurer, 2004*a*,*b*). The role that the basic clusters, building both the structure of QC and AC, may play during a phase transition has also mostly been neglected. Simple model structures based on Penrose tilings decorated with just one type of atom are still in use. Also, no attention has been paid to the question whether or not fundamental differences exist in the mechanism of phase transitions from and to icosahedral and decagonal QC due to different geometrical constraints.

Geometrical models of mechanisms of phase transitions from quasiperiodic to periodic structures based on the periodic average structure (PAS) (Steurer & Haibach, 1999*a*) common to both the QC and the AC were developed by Steurer (1999, 2000*a*,*b*) and studied in simulations by Honal *et al.* (1998). In their two-step model for the decagonal QC–AC transformation, first a partially disordered approximant domain structure results rapidly from small atomic displacements. Subsequently, atomic diffusion leads rather slowly to an ordered AC. The basic idea behind this approach is to describe the structure of a QC as IMS (Steurer, 2000*b*). This allows the *n*D description of a QC–AC transition with a similar simplicity to that for IMS.

In the example of a 1D quasicrystal (Fibonacci chain, see Fig. 4), it was shown how nanodomain structures (Steurer, 1999; Honal *et al.*, 1998) and modulated QC structures (Steurer, 2000*b*) evolve in a first step. Close to the transition temperature, AC nuclei begin to grow everywhere in the QC matrix where locally the structures of the QC and its $\langle n, m\rangle$ approximant are already very similar. These regions are around the origin (0,0) and all hyperlattice points of the type (F_{k+1},F_k). For special values of k where $F_{k+2} = l(n + m)$, with $l \in Z$, all $\langle n,m\rangle$ AC unit cells are in-phase (*i.e.* on the same AC lattice) and have their origins at hyperlattice points (F_{k+1}, F_k). This condition is fulfilled for multiples of k because $F_{lk} = LF_k$, with integer L and $l = 1, 2, \ldots$ (Huang & Gong, 1998). Since n, m correspond to subsequent Fibonacci numbers $n = F_{k'+1}$, $m = F_{k'}$, the period of the rational $\langle n, m\rangle$ AC unit cell along $\mathbf{V}^{\|}$ corresponds to $(n + m)a_{\rm av}^{\rm FS} = F_{k'+2}a_{\rm av}^{\rm FS}$, with the lattice parameter of the PAS of the Fibonacci chain. Thus, all approximant domains growing from nuclei located at positions of that kind are in-phase. This explains why domains being far away from each other can be in-phase as observed in decagonal Al–Co–Ni transformation products (Kalning *et al.*, 1997).

The nuclei, consisting of a few AC unit cells, are chemically well ordered and their PAS coincide with that of the QC (Fig. 3*a*). With increasing size of the AC domains, however, the interatomic distances of the AC have to be slightly modified to keep the density constant over the whole sample (Fig. 3*b*). Thus, the AC domains are strained. The strain can be partly released by the formation of $\langle n + 1, m + 1\rangle$ AC domain walls.

Further grain coarsening allows the strain to be released and to relax the interatomic distances to their former values (Fig. 3*c*). The registry of AC unit cells on the lattice of the PAS forces the formation of low-energy domain boundaries or even a smooth transition from one domain to the other. The AC domains themselves, however, show a kind of chemically modulated structure (antiphase subdomains, see also Fig. 4). This is a result of the superposition of a completed positional QC–AC transformation with the chemical order of the original QC. A well ordered AC could be obtained from this transition state only by diffusion processes during long-time annealing. The diffraction pattern of the transient shown schematically in Fig. 3(*a*) would be very similar to that of the QC plus some diffuse scattering. With larger AC domains (Fig. 3*b*), broad AC reflections would replace more and more QC reflections and the diffuse scattering would become more structured. Finally (Fig. 3*c*), sharp AC reflections accompanied by (diffuse) satellite reflections plus some less structured diffuse scattering would be observed.

The results obtained for the 1D QC, however, cannot all be simply transferred to decagonal or icosahedral QC. For them, such simple one-to-one mappings of all atoms of the PAS of QC and AC are not possible. Consequently, the first step in a QC-to-AC transformation in this model would yield a much more disordered intermediate state and, in the second step, diffusion would play an important role to reach the thermodynamic equilibrium state. This was demonstrated in the case of a model structure for *d*-Al–Co–Ni, where the specific properties of its PAS cause inherent disorder and the need of diffusion of approximately 40% of all atoms in the course of the second stage of the QC-to-AC transformation (Honal *et al.*, 1998).

However, at least in the case of decagonal phases, 1D quasicrystals have been observed as intermediate states of the QC–AC transition. Probably, they generally play a role as intermediate state in the QC–AC transitions. Rochal & Lorman (2003) proposed an interesting two-step mechanism for a 'continuous defect-free structural transformation of long-range order' of the infinite pentagonal Penrose tiling to one of its orthorhombic approximants through a series of intermediate structures, one of them a 1D quasicrystal. It essentially works by applying 1D linear phason strain in combination with a simultaneous variation of the shape of the atomic surfaces in the higher-dimensional description. This is done twice in two mutually orthogonal directions. In the case of finite samples, the result cannot be free of defects since insufficient or excess vertices have to come from or go to infinity. Nothing is said about how chemical ordering is achieved.

An aspect related to that of the PAS of QC (Steurer & Haibach, 1999*a*) was pointed out by Rochal (1999*b*) and Rochal & Lebedyuk (2000). In the example of an octagonal structure, the relationship between the vertices of the quasiperiodic structure resulting from the averaging of two square lattices to the generating periodic structures was discussed. A QC–AC transformation can then be described by a continuous deformation of the generating lattices.

Another quasicontinuous mechanism is based on the so-called *T* lattice (incommensurate to the AC lattice), of which at least a subset is left invariant during the transition QC to AC (Rochal *et al.*, 1996; Rochal, 1997, 1999*a*). The order parameters are related to the amplitudes of the QC and AC basic mass density waves. The local structure of the QC and AC is similar close to the *T* lattice points allowing a continuous QC-to-AC transformation by small displacements of atoms. Farther away from the *T* lattice points, atomic diffusion is necessary. If no relaxation takes place during the diffusion process, the quasiperiodic long-range order would be preserved. This means that, in an X-ray experiment, no reflection splitting would be seen after the QC-to-AC transition in contradiction to what has been already observed.

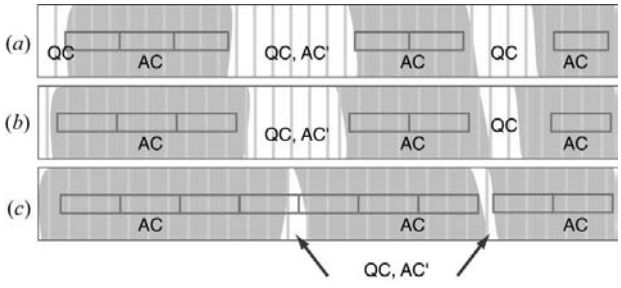

Figure 3
Scenario of a QC–AC transformation. The AC domains are shadowed, the AC unit cells are schematically drawn, and the lattice of the PAS is shown by vertical grey lines. The different stages of the transition are shown from top to bottom: In (*a*), the PAS (and therewith the point densities) of QC and AC regions are equal; in (*b*), the AC domains relax their PAS, and the remaining QC or AC′ matrix acts as discommensuration with respect to the AC lattice. In (*c*), the final fully relaxed state with low-energy domain boundaries is shown. The arrows indicate a unit-cell misfit of one period of the PAS (Steurer, 1999).

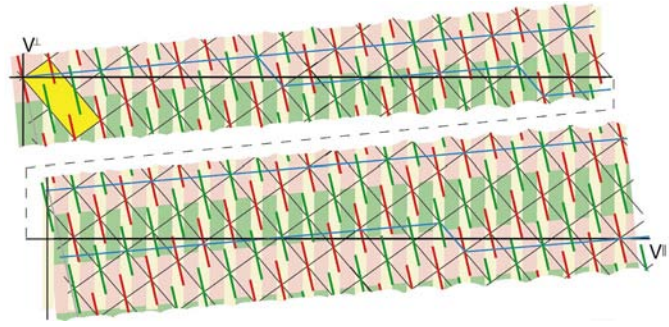

Figure 4
The phase transition from the two-colour Fibonacci chain to the ⟨2,1⟩ approximant in the IMS setting. The vertices of the 1D quasiperiodic structures are generated where the physical space (black horizontal line) cuts the 2D hypercrystal. The straight blue line indicates the cutting space globally generating a ⟨2,1⟩ approximant. The stepped blue line runs closely around $V^{\|}$ and represents the cutting space to generate locally nuclei of ⟨2,1⟩ approximants separated by discommensurations. In the lower part of the drawing, the continuation of the upper part is schematically indicated. The light red and green fields in the background illustrate the in-phase and anti-phase domains: if $V^{\|}$ and the cutting space of the approximant (blue line) are both within a one-coloured field, an in-phase domain results, otherwise an anti-phase domain results (Steurer, 2000*b*).

A somewhat different approach was used by Rochal & Lebedyuk (1998) and Rochal *et al.* (1999). The QC-to-AC transformation was geometrically achieved by linear continuous inhomogeneous strain without the need of any atomic jumps (phason flips). The authors point out, however, that this strain field should only be considered as an order parameter and not as a microscopic model for the actual displacements of the atoms.

The Gorsky–Bragg–Williams theory has its focus on the microscopic structural factors governing a phase transition. It works quite well for the atomic ordering in structures with two equivalent sublattices such as CsCl-type structures. Chizhikov (2000) modified it for structures with dodecahedral local order as is observed in QC and AC. This approach may be used for describing ordering phenomena in QC such as the transition from the *F*- to the *F*2-type phase in *i*-Al–Mn–Pd.

4. Concluding remarks

An important problem is that most of the present experimental information on QC phase transitions is only qualitative. Even so, elementary information on whether a phase transition is of first or second order is rarely available. This makes theoretical modelling sometimes somewhat arbitrary. A prerequisite for quantitative data would be studying well characterized samples only. In the case of stable QC for starting materials, they should be sufficiently thermally equilibrated at any temperature studied. These seem to be quite self-evident requirements, however, they are by no means easy to achieve. QC characterization is extremely intricate and equilibration can be extremely time consuming. At temperatures below approximately half of the melting temperature, equilibration may take months at least.

There is now some progress in the understanding of phase transitions from and to QC. In particular, *n*D modelling proved to be a powerful tool for interpreting on the atomic scale the formation of intermediate states such as modulated QC. However, as long as fundamental questions about stability and structure of QC are still open (see, for instance, Steurer, 2004*a*), final answers cannot be given about the mechanism of the transformations from and to this at present not well defined state.

Financial support by Swiss National Science Foundation (NF 2000-067872.02/1) is gratefully acknowledged.

References

Abe, E. & Tsai, A. P. (1999). *Phys. Rev. Lett.*, **83**, 753–756.

Akahama, Y., Mori, Y., Kobayashi, M., Kawamura, H., Kimura, K. & Takeuchi, S. (1989). *J. Phys. Soc. Jpn*, **58**, 2231–2234.

Asahi, N., Noguchi, S. & Matsumura, K. (1994). *Mater. Sci. Eng.* A**181/182**, 819–822.

Audier, M., Bréchet, Y., De Boissieu, M., Guyot, P., Janot, C. & Dubois, J. M. (1991). *Philos. Mag.* B**63**, 1375–1393.

Audier, M., Bréchet, Y. & Guyot, P. (1990). *Philos. Mag. Lett.* **61**, 55–62.

Audier, M., Duneau, M., De Boissieu, M., Boudard, M. & Letoublon, A. (1999). *Philos. Mag.* A**79**, 255–270.

Audier, M., Guyot, P., De Boissieu, M. & Menguy, N. (1993). *J. Non-Cryst. Solids*, **153 and 154**, 591–594.

Audier, M. & Robertson, B. (1991). *Philos. Mag. Lett.* **64**, 401–409.

Baake, M., Joseph, D. & Kramer, P. (1991). *J. Phys. A*, **24,** L961–L967.

Bak, P. (1982). *Rep. Prog. Phys.* **45**, 587–629.

Bak, P. (1985). *Phys. Rev. B*, **32**, 5764–5772.

Bancel, P. A. (1989). *Phys. Rev. Lett.* **63**, 2741–2744.

Beraha, L., Steurer, W. & Perez-Mato, J. M. (2001). *Z. Kristallogr.* **216**, 573–585.

Bokhonov, B. B., Ivanov, E. Y., Tolochko, B. P. & Sharaphutdinov, M. P. (2000). *Mater. Sci. Eng.* A**278**, 236–241.

Bolliger, B., Erbudak, M., Vvedensky, D. D. & Zurkirch, M. (1998). *Phys. Rev. Lett.* **80**, 5369–5372.

Boudard, M., Letoublon, A., De Boissieu, M., Ishimasa, T., Mori, M., Elkaim, E. & Lauriat, J. P. (2000). *Mater. Sci. Eng.* A**294**–**296**, 217–220.

Chen, L. F., Wang, L. M., Guo, Y. X., & Ewing, R. C. (1997). *Nucl. Instrum. Methods Phys. Res. B*, **127**, 127–131.

Chizhikov, V. A. (1999). *Crystallogr. Rep.* **44**, 1024–1029.

Chizhikov, V. A. (2000). *Crystallogr. Rep.* **45**, 122–127.

Coddens, G., Dunlop, A., Dammak, H., Chatterjee, R., Calvayrac, Y., Quiquandon, M., Elkaim, E., Gailhanou, M. & Rouziere, S. (2003). *Nucl. Instrum. Methods Phys. Res. B*, **211**, 122–132.

Cummins, H. Z. (1990). *Phys. Rep.* **185**, 211–409.

De Boissieu, M., Boudard, M., Ishimasa, T., Elkaim, E., Lauriat, J. P., Letoublon, A., Audier, M., Duneau, M. & Davroski, A. (1998). *Philos. Mag.* A**78**, 305–326.

Denoyer, F., Launois, P., Motsch, T. & Lambert, M. (1993). *J. Non-Cryst. Solids*, **153 and 154**, 595–599.

Denoyer, F., Reich, R. & Lauriat, J. P. (2000). *Mater. Sci. Eng.* A**294**, 287–290.

Döblinger, M., Wittmann, R., Gerthsen, D. & Grushko, B. (2002). *Phys. Rev. B*, **65**, 224201.

Duneau, M. (1992). *J. Phys. (Paris) I* , **2**, 1731–1740.

Duneau, M. & Oguey, C. (1990*a*). *J. Phys. (Paris)*, **51**, 5–19.

Duneau, M. & Oguey, C. (1990*b*). *Europhys. Lett.* **13**, 67–72.

Duneau, M., & Oguey, C. (1991). *J. Phys. A*, **24**, 461–475.

Edagawa, K., Sawa, H. & Takeuchi, S. (1994). *Philos. Mag. Lett.* **69**, 227–234.

Fettweis, M., Launois, P., Denoyer, F., Reich, R. & Lambert, M. (1994). *Phys. Rev. B*, **49**, 15573–15587.

Fettweis, M., Launois, P., Reich, R., Wittmann, R. & Denoyer, F. (1995). *Phys. Rev. B*, **51**, 6700–6703.

Frank, F. C. (1952). *Proc. R. Soc. London Ser. A*, **215**, 43–46.

Gittus, J. (1978). *Irradiation Effects in Crystalline Solids*. London: Applied Science.

Hassdenteufel, K., Krauss, G. & Steurer, W. (2004). Personal communication.

Hirai, I., Ishimasa, T., Létoublon, A., Boudard, M. & De Boissieu, M. (2000). *Mater. Sci. Eng.* A**294–296**, 33–36.

Holzer, J. C. & Kelton, K. F. (1993). *Crystal–Quasicrystal Transitions*, edited by M. J. Yacaman & M. Torres, pp. 103–142. Amsterdam: North-Holland.

Honal, M., Haibach, T. & Steurer, W. (1998). *Acta Cryst.* A**54**, 374–387.

Hu, C. Z., Wang, R. H., Ding, D. H. & Yang, W. G. (1996). *Phys. Rev. B*, **53**, 12031–12034.

Huang, X. & Gong, C. (1998). *Phys. Rev. B*, **58**, 739–744.

Ishi, Y. (1990). *Philos. Mag. Lett.* **62**, 393–397.

Ishi, Y. (1992). *Phys. Rev. B*, **45**, 5228–5239.

Ishimasa, T. (1995). *Philos. Mag. Lett.* **71**, 65–73.

Janot, C., Audier, M., De Boissieu, M. & Dubois, J. M. (1991). *Europhys. Lett.* **14**, 355–360.

Janssen, T. (1991). *Europhys. Lett.* **14**, 131–136.

Jiang, J. Z., Zhuang, Y. X., Rasmussen, H., Saida, J. & Inoue, A. (2001). *Phys. Rev. B*, **64**, 094208.

Kalning, M., Kek, S., Krane, H. G., Dorna, V., Press, W. & Steurer, W. (1997). *Phys. Rev. B*, **55**, 187–192.

Kelton, K. F. (2004). *J. Non-Cryst. Solids*, **334**, 253–258.
Kelton, K. F., Lee, G. W., Gangopadhyay, A. K., Hyers, R. W., Rathz, T. J., Rogers, J. R., Robinson, M. B. & Robinson, D. S. (2003). *Phys. Rev. Lett.* **90**, 195504.
Kim, D. H., Chattopadhyay, K. & Cantor, B. (1990). *Philos. Mag.* A**62**, 157–171.
Kimura, K., Hashimoto, T., Suzuki, K., Nagayama, K., Ino, H. & Takeuchi, S. (1986). *J. Phys. Soc. Jpn*, **55**, 534–543.
Kupsch, A., Meyer, D. C., Gille, P. & Paufler, P. (2002*a*). *J. Alloys Compounds*, **336**, 154–158.
Kupsch, A., Meyer, D. C., Gille, P. & Paufler, P. (2002*b*). *J. Alloys Compounds*, **342**, 256–260.
Le Lann, A. & Devaud, J. (2000). *Eur. Phys. J.* B**15**, 235–246.
Letoublon, A., Ishimasa, T., De Boissieu, M., Boudard, M., Hennion, B. & Mori, M. (2000). *Philos. Mag. Lett.* **80**, 205–213.
Li, F. H. & Cheng, Y. F. (1996). *Chin. Phys. Lett.* **13**, 199–202.
Liu, L. & Chan, K. C. (2004). *J. Alloys Compounds*, **364**, 146–155.
Liu, W. & Köster, U. (1993). *J. Non-Cryst. Solids*, **153 and 154**, 615–619.
Liu, W., Köster, U. & Zaluska, A. (1991). *Phys. Status Solidi*, **126**, K9–K14.
Ma, L., Kuo, K. H. & Wang, R. (1990). *J. Less-Common Met.* **163**, 37–49.
Mai, Z. H. I, Xu, L., Wang, N., Kuo, K. H., Jin, Z. C. & Cheng, G. (1989). *Phys. Rev. B*, **40,** 12183–12186.
Menguy, N., Audier, M. & Guyot, P. (1992). *Philos. Mag. Lett.* **65**, 7–14.
Menguy, N., De Boissieu, M., Guyot, P., Audier, M., Elkaim, E. & Lauriat, J. P. (1993). *J. Phys. (Paris) I*, **3**, 1953–1968.
Misra, D. K., Tiwari, R. S. & Srivastava, O. N. (2003). *Phys. Status Solidi A*, **200**, 326–332.
Mukhopadhyay, N. K., Murthy, G. V. S., Murty, B. S. & Weatherly, G. C. (2002*a*). *Philos. Mag. Lett.* **82**, 383–392.
Mukhopadhyay, N. K., Murthy, G. V. S., Murty, B. S. & Weatherly, G. C. (2002*b*). *J. Alloys Compounds*, **342**, 38–41.
Mukhopadhyay, N. K., Yadav, T. P. & Srivastava, O. N. (2002). *Philos. Mag.* A**82**, 2979–2993.
Nasu, S., Miglierini, M., Ishihara, K. N. & Shingu, P. H. (1992). *J. Phys. Soc. Jpn*, **61**, 3766–3772.
Pannetier, J., Dubois, J. M., Janot, C. & Bilde, A. (1987). *Philos. Mag.* B**55**, 435–457.
Perez-Mato, J. M. & Elcoro, L. (1994). *J. Phys. (Paris) I*, **4**, 1341–1352.
Qin, Y. L., Wang, R. H., Wang, Q. L., Zhang, Y. M. & Pan, C. X. (1995). *Philos. Mag. Lett.* **71**, 83–90.
Quivy, A., Quiquandon, M., Calvayrac, Y., Faudot, F., Gratias, D., Berger, C., Brand, R. A., Simonet, V. & Hippert, F. (1996). *J. Phys. Condens. Matter*, **8**, 4223–4234.
Reyes-Gasga, J., Garcia, R. & Jose-Yacaman, M. (1995). *Radiat. Phys. Chem.* **45**, 283–291.
Reyes-Gasga, J., Lara, A., Riveros, H. & Jose-Yacaman, M. (1992). *Mater. Sci. Eng.* A**150**, 87–99.
Ritsch, S., Beeli, C., Nissen, H. U., Godecke, T., Scheffer, M. & Lück, R. (1998). *Philos. Mag. Lett.* **78**, 67–75.
Rochal, S. B. (1997). *Crystallogr. Rep.* **42**, 714–723.
Rochal, S. B. (1999*a*). *Phys. Lett.* A**253**, 327–332.
Rochal, S. B. (1999*b*). *Phys. Rev. B*, **60**, 12687–12691.
Rochal, S. B., Dmitriev, V. P., Lorman, V. L. & Toledano, P. (1996). *Phys. Lett.* A**220**, 111–116.
Rochal, S. B. & Lebedyuk, I. V. (1998). *Phys. Lett.* A**250**, 152–156.
Rochal, S. B. & Lebedyuk, I. V. (2000). *Crystallogr. Rep.* **45**, 473–478.
Rochal, S. B., Lebedyuk, I. V. & Kozinkina, Y. A. (1999). *Phys. Rev. B*, **60**, 865–873.
Rochal, S. B. & Lorman, V. L. (2003). *Phys. Rev. B*, **68**, 4203–4203.
Sadoc, A., Itie, J. P., Polian, A. & Lefebvre, S. (1996). *Philos. Mag.* A**74**, 629–639.
Sato, K., Baier, F., Sprengel, W., Würschum, R. & Schaefer, H. E. (2004). *Phys. Rev. Lett.* **92**, 7403–7403.
Smith, D. J. (1997). *Rep. Prog. Phys.* **60**, 1513–1580.
Soltmann, C., Beeli, C., Luck, R. & Gander, W. (2003). *J. Appl. Cryst.* **36**, 1030–1039.
Song, S. G., Ryba, E. R. & Gray, G. T. (1996). *Mater. Sci. Eng.* A**219**, 66–70.
Song, S. H., Wang, L. & Ryba, E. R. (1993). *J. Mater. Sci. Lett.* **12**, 80–83.
Steurer, W. (1999). *MRS Proc.* **553**, 159–170.
Steurer, W. (2000*a*). *Mater. Sci. Eng.* A**294**, 268–271.
Steurer, W. (2000*b*). *Z. Kristallogr.* **215**, 323–334.
Steurer, W. (2004*a*). *J. Non-Cryst. Solids*, **334**, 137–142.
Steurer, W. (2004*b*). *Z. Kristallogr.* **219**, 391–446.
Steurer, W., Cervellino, A., Lemster, K., Ortelli, S. & Estermann, M. A. (2001). *Chimia*, **55**, 528–533.
Steurer, W. & Haibach, T. (1999*a*). *Acta Cryst.* A**55**, 48–57.
Steurer, W. & Haibach, T. (1999*b*). *Physical Properties of Quasicrystals*, edited by Z. Stadnik, pp. 51–90. Heidelberg/New York: Springer Verlag.
Steurer, W. & Haibach, T. (2001). *International Tables for Crystallography*, Vol. B, edited by U. Shmueli, pp. 486–518. Dordrecht: Kluwer Academic Publishers.
Tamura, R., Edagawa, K., Aoki, C., Takeuchi, S. & Suzuki, K. (2003). *Phys. Rev. B*, **68**, 174105.
Tamura, R., Murao, Y., Takeuchi, S., Ichihara, M., Isobe, M. & Ueda, Y. (2002). *Jpn. J. Appl. Phys.* **41**, L524–L526.
Toledano, P. & Dmitriev, V. (1996). *Reconstructive Phase Transitions: in Crystals and Quasicrystals*. Singapore: World Scientific.
Tsai, A. P., Hiraga, K., Inoue, A., Masumoto, T., Satoh, K., Tsuda, K. & Tanaka, M. (1994). *Mater. Sci. Eng.* A**182**, 750–753.
Tsai, A. P., Inoue, A. & Masumoto, T. (1987). *Jpn. J. Appl. Phys.* **26**, L1994–L1996.
Wang, N. & Kuo, K. H. (1990). *Philos. Mag. Lett.* **61**, 63–68.
Wang, Z., Yang, X. & Wang, R. (1993). *J. Phys. Condens. Matter*, **5**, 7569–7576.
Waseda, A., Kimura, K. & Ino, H. (1993). *Mater. Trans. Jpn. Inst. Met.* **34**, 169–177.
Waseda, A., Kimura, K. & Ino, H. (1994). *Mater. Sci. Eng.* A**182**, 762–765.
Winters, R. & Hammack, W. S. (1993). *Science*, **260**, 202–204.
Xu, L., Wang, N., Lee, S. T. & Fung, K. K. (2000). *Phys. Rev. B*, **62**, 3078–3082.
Yacaman, M. J. & Torres, M. (1993). Editors. *Crystal–Quasicrystal Transitions.* Amsterdam: North-Holland.
Yang, X. X., Wang, R. H. & Fan, X. J. (1996). *Philos. Mag. Lett.* **73**, 121–127.
Yi, S. & Kim, D. H. (2000). *J. Mater. Res.* **15**, 892–897.
Zhang, H. & Urban, K. (1992). *Philos. Mag. Lett.* **66**, 209–215.